Article:
Amariutei, O.A., Ramsdale-Capper, R., Correa Álvarez, M. et al. (2018) Modelling the properties of a difunctional epoxy resin cured with aromatic diamine isomers. Polymer, 156. pp. 203-213. ISSN: 0032-3861

https://doi.org/10.1016/j.polymer.2018.10.016

Polymer 156 (2018) 203–213

Contents lists available at ScienceDirect

Polymer

journal homepage: www.elsevier.com/locate/polymer

Modelling the properties of a difunctional epoxy resin cured with aromatic diamine isomers

Olga A. Amariutei, Roderick Ramsdale-Capper, Mariana Correa Álvarez, Louise K.Y. Chan, Joel P. Foreman*

Department of Materials Science & Engineering, Sir Robert Hadfield Building, University of Sheffield, Sheffield, S1 3JD, UK

HIGHLIGHTS

- Group Interaction Modelling (GIM) is used to predict the properties of two isomeric DGEBA/DDS epoxy resins.
- The loss tangent profile, density and compressive stress-strain curves are measured both experimentally and predicted.
- Differences between *meta* and *para* isomers are successfully modelled and discussed in terms of molecular motions present.
- Experimental variation of the amine/epoxy ratio reveals subtle influences on the secondary phase transitions.

ARTICLE INFO

Keywords:
Group interaction modelling
Epoxy
DGEBA
DDS
Dynamic mechanical analysis

ABSTRACT

Group Interaction Modelling has been extended to predict a range of thermo-mechanical properties of diglycidyl ether of bisphenol A cured with two isomers of diaminodiphenyl sulphone. The *meta-meta* and *para-para* positions of the substituents on the phenylene rings in the curing agent cause differences in packing efficiency, reaction kinetics and conformational freedom. Experimental data in the form of dynamic mechanical, static mechanical and density measurements are acquired in order to provide validation for the model. The model has proven capable of accurately reproducing the experimental measurements to well within experimental errors in most cases. Both the experimental measurements and model predictions have highlighted a number of subtle differences in behaviour of the resins cured with the two diamine isomers. In particular, variation of the amine/epoxy ratio has revealed how the secondary phase transitions of the resins are influenced. Variation of the glass and beta transitions in amine rich, stoichiometric or epoxy rich mixtures is described in terms of the molecular motions responsible for the transitions and the underlying network structural differences between the *meta* and *para* isomers.

1. Introduction

The chemistry of epoxy resins is distinctive among thermosetting resins. Manipulations of the chemical structure and polymerisation process allow epoxy resins to span a wide range of mechanical properties, from relatively flexible to very stiff and relatively soft to very hard. Their versatility and broad range of available properties guarantees their continued use in various industries ranging from aerospace to adhesives. Traditionally, the epoxy resin development is accomplished through the use of expensive trial-and-error based experimental programs or relatively time-consuming theoretical models. A pragmatic model that allows the rapid yet accurate prediction of epoxy resin properties as a function of chemistry, temperature, strain and strain rate has the potential to revolutionise the route taken to new and improved epoxy resins. Group Interaction Modelling (GIM), conceived by David Porter in 1995, is one such model [1]. Initially, GIM was developed as a tool for predicting the properties of thermoplastics [2,3], but has since been extended to work with silks [4] and composites [5–7].

GIM has also been successfully used to predict the properties of highly crosslinked thermosetting polymers, such as the previously mentioned amine cured epoxy resins [8–10]. In particular, the incorporation of crosslinking into the model by reducing the available degrees of freedom has allowed the accurate prediction of cured epoxy resin properties. Elastic properties are predicted via a small number of input parameters based on the polymer's representative mer unit as a function of temperature. The loss events associated with the glass

* Corresponding author.
E-mail address: j.foreman@sheffield.ac.uk (J.P. Foreman).

https://doi.org/10.1016/j.polymer.2018.10.016
Received 13 July 2018; Received in revised form 14 September 2018; Accepted 7 October 2018
Available online 08 October 2018
0032-3861/

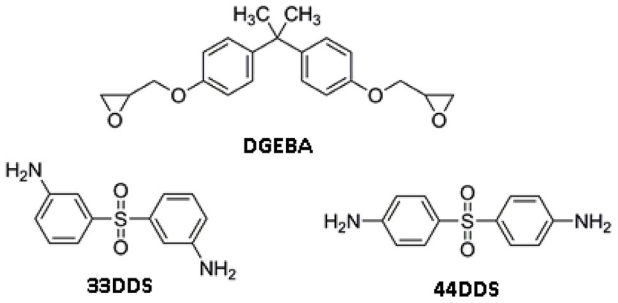

Fig. 1. Chemical structures of DGEBA, 33DDS and 44DDS.

transition and other sub-glass transitions are characterised and applied to the elastic properties to provide predicted viscoelastic properties. The strain rate dependence of the molecular motions responsible for the secondary phase transitions results in strain rate dependence of the predicted viscoelastic properties. Whilst previous modelling work in this area has concentrated on using aromatic amines to cure a variety of epoxies, GIM has also been successfully applied to a wide variety of aliphatic amine cured epoxy resins [11].

The default high performance epoxy resin, diglycidyl ether of bisphenol A (DGEBA), is used in a wide variety of applications, including as the matrix phase in composite systems. Part of the reason for this is the aromatic chain backbone (see Fig. 1) which improves stiffness and strength. When cured with an aromatic diamine, such as diaminodiphenyl sulphone (DDS), the properties of the resultant cured epoxy resins are much sought after, including a glass transition temperature approaching 200 °C and excellent chemical resistance. The cure reaction releases no volatiles and the cure shrinkage is minimal, all of which results in a highly desirable set of resin properties.

DDS specifically intended for curing epoxy resins is available as two different isomers where the substituents on the two phenylene rings are either in a *meta-meta* or a *para-para* arrangement. These are 3,3′-diaminodiphenyl sulphone (33DDS) and 4,4′-diaminodiphenyl sulphone (44DDS) respectively with structures shown in Fig. 1. Epoxy resins cured with these two diamine isomers differ in their properties in a relatively subtle fashion. Both DGEBA and triglycidyl aminophenol (TGAP) cured with 33DDS and 44DDS show internal antiplasticisation when using the *meta* compared to the *para* amine [12–14]. The results of these previous works suggest the internal antiplasticisation is caused by a combination of changes in packing efficiency, reaction kinetics and conformational freedom.

While GIM has been successfully applied to a trifunctional and tetrafunctional epoxy resin cured with 44DDS [8], we are not aware of any work in which GIM has been applied to a difunctional epoxy resin cured with two isomeric diamines. Therefore, the intention of this work is to apply GIM to DGEBA cured with both 33DDS and 44DDS. On initial inspection of the chemical structures, the two isomers of DDS vary only in the position of the substituents on the phenylene rings. The model is versatile enough to allow the two isomers to be parameterised, but whether the influence of switching isomers can be accurately captured by GIM remains to be seen. The internal antiplasticisation effect is complicated and a number of contributory factors govern its influence on resin properties. Previous work has shown that differences in the reactivity of the two isomers leads to differences in the degree cross-linking in the cured resin [14]. GIM does not natively model the cure reaction so it will be unable to capture this behaviour, however it should be able to predict the properties of the cured resin at the end of the reaction.

Alongside the model predictions, a series of experimental measurements will be made, primarily for model validation but also to provide insight into any subtle differences observed between the resins cured with the two isomers of DDS. Dynamic mechanical analysis (DMA) will measure the loss tangent profile to characterise the secondary phase transitions, gas pycnometry will measure the density to characterise the packing efficiency and compressive stress-strain curves will characterise the response to an applied static force.

2. Group interaction modelling

Group Interaction Modelling (GIM) is based upon the premise that the macroscopic mechanical response of a polymers is a direct consequence of energy stored and dissipated at the molecular level during thermo-mechanical loading [2,3,15–17]. The energetic description for the deformation mechanisms of polymers originates in the works of Eyring [18], Ferry and Myers [19], and Bauwens-Crowet [20]. Unlike atomistic models, which map the exact location of every atom in the system of interest, GIM uses an ensemble average approach for the definition of the polymer. The 3D network nature of cured epoxy resins means there is an inherent uncertainty as to their exact chemical structure and, as such, a model that eliminates the need for such information is advantageous. In GIM, rather than Cartesian (or similar) coordinates of each atom in a representative section of the polymer, the entire polymer is defined in terms of the functional groups present. So, the number and type of each functional group present in the polymer's mer unit is enough information to parameterize the model. In an averaged approach such as presented here, information on the connectivity between individual functional groups is not necessary, particularly for an isotropic, single phase epoxy resin.

GIM uses a mean–field potential function approach to predict the thermal, volumetric and mechanical properties of polymers. The method uses a simple contribution based approach to calculate the total energy of the system. The model assumes an ideal hexagonal arrangement of six polymer chains around a central chain, from which any non-ideal behaviour can be determined (e.g. reductions in crystallinity). Interactions between neighbouring polymer chains are defined using a potential function (Equation (1)) that consists of several thermodynamic energy terms and which represents the equation of state for the system.

$$E_{total} = E_{coh}\left(\left(\frac{V_T}{V}\right)^6 - 2\left(\frac{V_T}{V}\right)^3\right) = -E_{coh} + H_C + H_T + H_M \tag{1}$$

The total energy of the system, E_{total}, is expressed as a potential energy well of depth, E_{coh}, where E_{coh} is the 0 K cohesive energy for the system. The expression is based upon the standard Lennard–Jones potential function but reformulated in terms of the volume, V. In GIM, the polymer is assumed to be much longer than its other two perpendicular dimensions so therefore $V \propto r^2$, where r is the inter-chain separation distance. The volume is parameterised via the van der Waal's volume of each mer unit, V_w, and determined by solving Equation (1). Density can be calculated from the volume and molecular mass, M.

In bulk thermodynamic terms, the total energy is comprised of cohesive energy (E_{coh}), configurational energy (H_C), thermal energy (H_T) and mechanical energy (H_M). The cohesive energy, E_{coh}, represents the attractive forces holding the polymer chains together, against which the following repulsive forces act. The configurational energy, H_C, represents how ordered the polymer is and will have a larger magnitude in crystalline systems and a correspondingly smaller magnitude in amorphous systems. The value is conveniently expressed as a fraction of the cohesive energy depending on the degree of crystallinity. The thermal energy, H_T, rises as increased molecular motion in the system occurs as a result of increasing the temperature. It can be quantified from the heat capacity of the system, C. The mechanical energy, H_M, is a term used to quantify changes in the system as a result of applied mechanical fields and is not normally required for simple property prediction.

In GIM, the heat capacity is used to capture the molecular level skeletal mode vibrations which govern the temperature dependent mechanical properties of the polymer. The temperature dependent heat capacity can then be integrated over temperature to provide the

thermal energy term, H_T. The total system heat capacity, C, is discretised into three terms as shown in Equation (2) where C_b, C_β and C_g are the heat capacities associated with the background, the beta transition and the glass transition respectively.

$$C = C_b + C_\beta + C_g \tag{2}$$

In polymer terms, the background heat capacity defines the elastic contribution to the total heat capacity. Similarly, the beta transition and glass transition heat capacities define the viscous contribution to the heat capacity through the molecular level loss events which each represent. When summed, the total heat capacity therefore, represents the full temperature dependent viscoelastic response of the polymer and can be used as the basis for the property predictions which follow. A one-dimensional Debye function of skeletal mode vibrations is used to describe the background heat capacity, C_b, in terms of the number of background degrees of freedom per group, N_b, the reference temperature of cooperative skeletal vibrations, θ_1, and the temperature, T. This is expressed in Equation (3) where R is the gas constant.

$$C_b = N_b R \frac{\left(\frac{6.7T}{\theta_1}\right)^2}{1+\left(\frac{6.7T}{\theta_1}\right)^2} \tag{3}$$

Parameterisation of the beta and glass transitions in GIM is described in detail in previous works [1,8]. Briefly, the glass transition temperature, T_g, is predicted using Equation (4) below which has contributions from both the chain stiffness (via θ_1) and a balance between attractive (E_{coh}) and repulsive forces (N). The resulting expression allows for the accurate prediction of the glass transition temperature from three relatively simple parameters obtained from the polymer chemical structure.

$$T_g = 0.224\theta_1 + \frac{0.0513E_{coh}}{N} \tag{4}$$

The total loss through the glass transition, $\tan\Delta_g$, is predicted using Equation (5) below where N_c is the degrees of freedom associated with the polymer chain (rules for estimating N_c are provided elsewhere [1]. This expression allows the magnitude of the glass transition to be quantified and therefore ensures that properties through and after the transition are accurately predicted.

$$\tan\Delta_g = 0.0085\frac{E_{coh}}{N_c} \tag{5}$$

In a similar vein, the beta transition temperature, T_β, is predicted using Equation (6) below where ΔH_β is the activation energy for the beta transition, $\dot{\varepsilon}$ is the strain rate and f is the characteristic frequency of skeletal group vibrations. The value of f is obtained from $k\theta_1 = hf$ where k is Planck's constant and h is Boltzmann's constant.

$$T_\beta = \frac{-\Delta H_\beta}{R\ln\left(\frac{\dot{\varepsilon}}{2\pi f}\right)} \tag{6}$$

The total loss through the beta transition, $\tan\Delta_\beta$, is predicted using Equation (7) below. Again, the accurate prediction of the total loss through the transition is critical as it allows the properties through and after the transition to be determined. In particular, the beta transition is a sub-ambient transition, so quantifying its magnitude is important for accurate property prediction at room temperature.

$$\tan\Delta_\beta = 25\frac{\Delta H_\beta}{N_c} \tag{7}$$

The degrees of freedom, N, is the most sensitive of the parameters in GIM and care must be taken in its evaluation. Initial values are taken from group contribution tables [1] though there are alternative approaches to its estimation [21]. The atoms within each functional group along the polymer backbone are assumed to act cooperatively, therefore requiring a value of N for each functional group. As each functional group is attached to the polymer backbone, their motion is restricted in this direction. This results in a default degrees of freedom for each functional group of $N = 2$. Combinations of functional groups will often have combined values of N, particularly where functional groups must act cooperatively, such as in phenylene rings. The addition of crosslinking into the model is achieved by reducing the value of N by 3 for each branching site on the mer unit. The fraction of un-crosslinked to crosslinked degrees of freedom is used in predicting the characteristics of the transitions. Each transition is assigned a specific contribution to the total degrees of freedom based on this fraction and the degree of cure.

Now that a prediction of the viscoelastic heat capacity has been obtained, a series of linked constitutive equations predicting the remaining properties are defined. The volumetric thermal expansion coefficient, α, can be calculated using Equation (8) below.

$$\alpha = \frac{1.38C}{RE_{coh}} \tag{8}$$

Using a process similar to that provided for the heat capacity in Equation (2), the elastic bulk modulus, B_e, is defined using Equation (9).

$$B_e = 18\frac{E_{total}}{V} \tag{9}$$

From this the viscoelastic tensile modulus, E_t, is defined in Equation (10) which incorporates the effects of the losses incurred through the glass and beta transitions.

$$E_t = B_e exp\left(\frac{-(\tan\Delta_g + \tan\Delta_\beta)}{AB_e}\right) \tag{10}$$

The term A is a geometric factor and is defined in Equation (11) where L is the mer unit length.

$$A = \frac{1.5\times10^{-5}L}{\theta_1 M} \tag{11}$$

The elastic strain, ε_e, can be determined by integrating the linear thermal expansion coefficient over temperature. The linear thermal expansion coefficient is approximately $^1/_3$ of the volumetric thermal expansion coefficient in isotropic polymers. This is then combined with the loss event information to provide the viscoelastic strain, ε, as shown in Equation (12). A series of tensile stresses are then defined for dummy temperatures using the strain and the tensile modulus. Poisson's ratio is determined using the bulk and elastic moduli and, lastly, compressive stress is calculated using Poisson's ratio to correct the tensile stress.

$$\varepsilon = \int \frac{\alpha}{3}dT\left(1 + \int(\tan\delta_g + \tan\delta_\beta)dT\right) \tag{12}$$

3. Experimental

The epoxy resin, diglycidyl ether of bisphenol A (DGEBA, supplied as Epikote 828 from Delta Resins Ltd.) is cured with either 3,3′-diaminodiphenyl sulphone (33DDS, supplied as Aradur 9719-1 from Huntsman Advanced Materials) or 4,4′-diaminodiphenyl sulphone (44DDS, supplied by Sigma Aldrich). The cured resins are hereafter referred to as DGEBA/33DDS and DGEBA/44DDS. Epikote 828 is used instead of pure DGEBA as it is easier to process. The chemical structure of Epikote 828 is given in Fig. 2 where it can be seen that the structures of the two resins are very similar when n = 0.1.

Based on the amine hydrogen equivalent weight of DDS (62 g.eq^{-1})

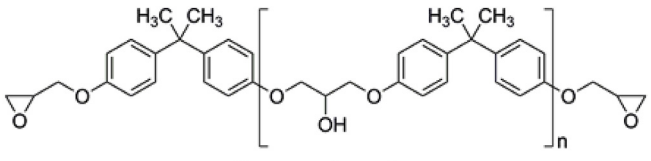

Fig. 2. Chemical structure of Epikote 828.

and the epoxy equivalent weight of Epikote 828 (approximately 187 g.eq^{-1}), the stoichiometric amine/epoxy ratio for Epikote 828 cured with DDS is 33.2:100. For the majority of the experiments and modelling presented in the following sections, an epoxy rich mixture of 30:100 is used instead. This is common in industry as it encourages maximum amine conversion limiting moisture uptake in the cured resin. For the stoichiometry variation section, another four experimental amine/epoxy weight ratios were used. These are approximately 36.5:100, 34.9:100, 33.2:100 and 31.6:100. In terms of molar ratios of amine groups to epoxy groups (henceforth termed amine/epoxy ratio), we have experimentally tested and modelled a total of 5 different amine/epoxy ratios. These are approximately 1:0.9, 1:0.95, 1:1, 1:1.05 and 1:1.1 which cover the range of amine rich, stoichiometric and epoxy rich ratios respectively.

The epoxy is weighed and heated to 80 °C in an oil bath and mechanically stirred with the amine hardener at 120 °C until a clear homogeneous solution is obtained. After 10 min degassing in a vacuum oven at 100 °C, the mixture is poured onto a treated, toughened glass plate which has been preheated to 100 °C. The curing schedule used was ramp to 120 °C at 2 °C.min^{-1}, dwell for 2 h, ramp to 185 °C at 2 °C.min^{-1}, dwell for 6 h, and finally a ramp down to 20 °C at 2 °C.min^{-1}. Test specimens for DMA and pycnometry were cut and polished. Samples for static compression testing were made using borosilicate glass test tubes (10 mm diameter) and machined to give parallel faces.

DMA testing was performed using a Perkin Elmer DMA8000 with the single cantilever geometry and a strain amplitude of 0.05 mm. Temperature scans were performed from approximately −160 °C to approximately 50 °C above the glass transition temperatures at a heating rate of 3 °C.min^{-1}. Loss tangent profiles were measured at 3 different frequencies, 1, 5, and 10 Hz. Transition temperatures were measured using OriginPro 8 software which is particularly effective in accurately determining the peak temperature of the very broad beta transition.

Gas pycnometry was performed using a Micrometrics AccupycII 1340. The volume of helium gas displaced at 19 psi over 25 cycles at approximately 27 °C provides an accurate measure of the sample volume. Density is then calculated from the sample mass measured on a four point balance.

Compression testing was performed using an Instron 5582 tensometer with an SFL environmental chamber to maintain a constant temperature of 30 ± 2 °C. The sample length was set at 9 ± 2 mm to limit buckling effects and strain rates of 1, 5 and 10 mm.min^{-1} were used. The sample faces were lightly coated with 100% petroleum jelly to reduce friction between the sample and the compression platens reducing barrelling effects. Strain was measured from the crosshead separation so a compliance correction was applied to the data. Compressive modulus measurements were calculated from the initial 0.05–0.25% strain and the yield strength was determined as the first maximum of the compression curve. At least five samples were tested at each strain rate. The data with the smallest deviation from the average was selected for compressive stress-strain comparison to GIM predictions.

4. Results and discussion

Assigned values of each of the GIM parameters (degrees of freedom, cohesive energy and van der Waal's volume) are given in Table 1. The functional group values are obtained from group contribution tables [1]. These are then summed to give values for the DGEBA, 33DDS and 44DDS mer units based on the chemical structures in Fig. 1. Finally, cured mer unit parameters are obtained by combining the mer unit parameters based on the stoichiometry of each resin investigated. The cured mer unit parameters are used as input into the GIM equations discussed earlier for the prediction of cured resin properties.

Table 1
GIM parameters for the functional groups, mer units and cured mer units. Values for the cured mer unit are for an amine/epoxy ratio of 1:1.1.

Functional Group	N	E_{coh} (J/mol)	V_w (cm^3/mol)
CH_n	2	4500	10.25
N	2	9000	4
CH(OH)	2	20,800	11.5
SO_2	2	45,000	20.3
O	2	6300	5
Epoxy	4	15,300	22
Phenylene Ring	3	25,000	43.3
Mer Unit	N	E_{coh} (J/mol)	V_w (cm^3/mol)
DGEBA	24	135,700	191.7
33DDS	14	113,000	114.9
44DDS	12	113,000	114.9
Cured Mer Unit	N	E_{coh} (J/mol)	V_w (cm^3/mol)
DGEBA/33DDS	21	130,460	173.9
DGEBA/44DDS	20	130,460	173.9

4.1. Loss tangent profiles

The loss tangent profiles for DGEBA/33DDS and DGEBA/44DDS are predicted using Equations (4)–(7) and measured using DMA. Comparisons of the experimental and GIM predicted profiles are shown in Figs. 3 and 4, which include magnifications of the lower temperature beta transitions for clarity. The plots show the loss tangent profiles for a frequency of 1 Hz, while the profiles at frequencies of 5 and 10 Hz are provided in the supplementary data. The 5 and 10 Hz plots are qualitatively similar to those for 1 Hz and are therefore provided for information only.

The comparisons between experimental and GIM predicted loss tangent profiles for DGEBA/33DDS and DGEBA/44DDS are good. The glass and beta transition temperatures are predicted well and the magnitude and shape of the loss peaks are generally in good agreement. Now that the overall gross features of the loss tangent profile are fully characterised by GIM, the loss event information can be applied to expressions defining the elastic behaviour of the polymer leading to predictions of the full viscoelastic response.

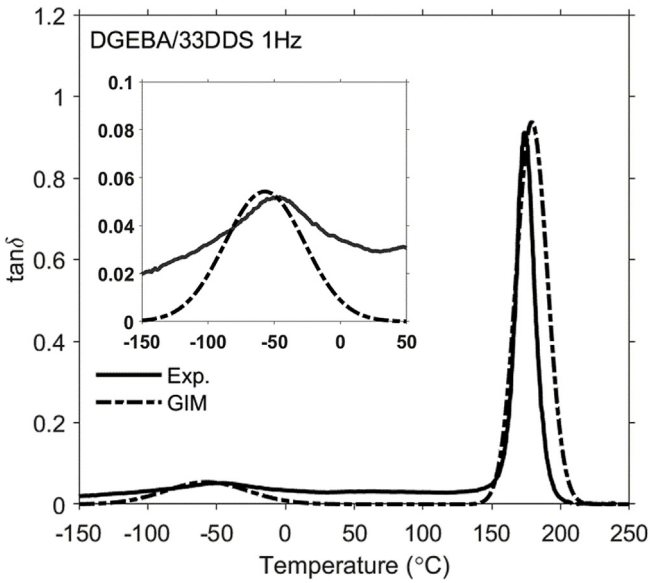

Fig. 3. Experimental and GIM loss tangent plots for DGEBA cured with 33DDS. The amine/epoxy ratio is 1:1.1 and the frequency is 1 Hz. The inset shows an enlargement of the beta transition in the −150 to 50 °C region.

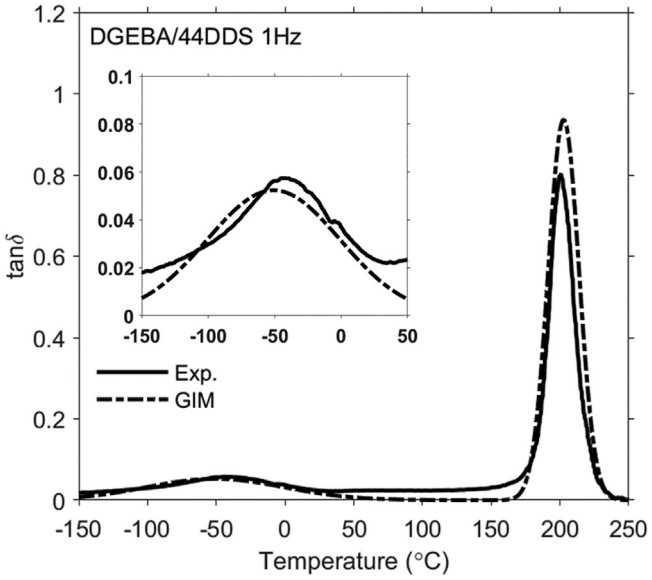

Fig. 4. Experimental and GIM loss tangent plots for DGEBA cured with 44DDS. The amine/epoxy ratio is 1:1.1 and the frequency is 1 Hz. The inset shows an enlargement of the beta transition in the −150 to 50 °C region.

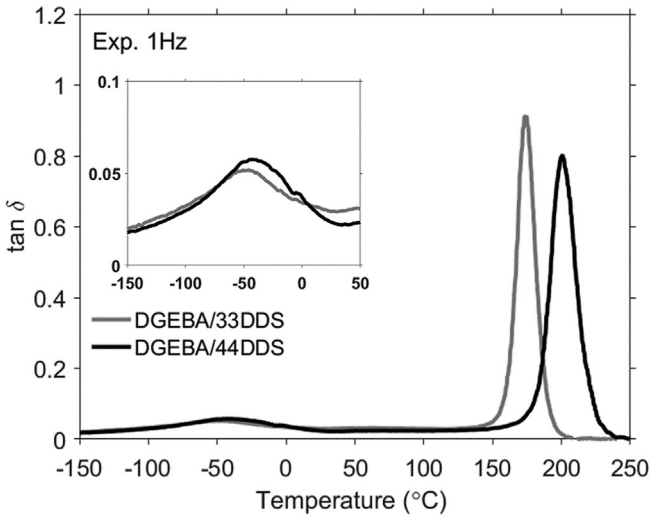

Fig. 5. Experimental loss tangent plots for DGEBA cured with 33DDS and 44DDS. The amine/epoxy ratio is 1:1.1 and the frequency is 1 Hz. The inset shows an enlargement of the beta transition in the −150 to 50 °C region.

The GIM implementation used in this work does not include a background loss function, which explains why the agreement between model and experiment is poorer at temperatures away from the two main transitions. This is a consequence of the approach used to account for loss in the model where the beta and glass transitions are explicitly defined, operate over a limited temperature range and are the only source of energy dissipation in the model. The inclusion of a background loss function to account for the relatively minor loss effects away from the main transitions is not technically difficult but has been neglected due to the limited impact it would have on the predicted properties. This effect appears more significant in the magnified beta transition plots in Figs. 3 and 4 where zero loss is predicted either side of the beta transition compared to a measured value of approximately 0.02. In between the two main transitions, the experimental background loss is typically approximately 0.01 and as such using zero background loss will have limited effect on predicted properties. Additionally, it is worth noting that while GIM under-predicts the loss tangent between the two main transitions, it also over-predicts the total loss through the glass transition, particularly on the hot side. These two effects will cancel to some extent further reducing the impact they have on the accuracy of predicted properties.

A comparison of the experimental loss tangent profiles for DGEBA/33DDS and DGEBA/44DDS is shown in Fig. 5. The difference in the glass transition temperatures is clear, DGEBA/44DDS has the higher peak temperature. This has been reported previously [12,13] and is a consequence of the higher crosslinking and chain stiffness in the *para* isomer. The beta transitions are similar in temperature and magnitude with small differences clearer in the magnified inset of Fig. 5. The higher temperature part of the beta transition peak is reduced in DGEBA/33DDS compared to DGEBA/44DDS. This confirms previous experiments and agrees with the proposed mechanism that the hot side of the peak is caused by phenylene ring rotation in the amine parts of the network. In the *meta* isomer, the ring rotation is restricted and hence the beta transition is supressed in this region.

Previous work [14] has shown that when triglycidyl-*para*-aminophenol (TGPAP) is cured with either 33DDS or 44DDS, a small, broad peak between the beta and glass transitions is observed in the loss tangent profile. This so-called 'omega transition' is thought to be caused by motions of larger segments of the structure [13,14] and often peaks between 50 and 100 °C. Typically, 33DDS cured resins have more pronounced omega transitions than 44DDS cured resins, though this effect is often obscured by overlap with the nearby beta transition. Fig. 3 shows a hint of a peak between 50 and 100 °C for DGEBA/33DDS but this is far less obvious than the omega peaks seen in TGPAP/DDS [14]. Fig. 4 shows there is no evidence of an omega transition peak in DGEBA/44DDS. Given the insignificance of the omega transition in DGEBA/DDS, no attempt is therefore made to model its effect on properties in this work.

The peak values of the experimental and GIM predicted beta and glass transition temperatures are given in Table 2 for three different frequencies, 1, 5 & 10 Hz. The agreement between the measured and predicted values is good across the three frequencies tested. The accuracy of the predicted value of either beta or glass transition for either DGEBA/33DDS or DGEBA/44DDS appears to deteriorate slightly as the frequency is increased. However, the difference between the experimental and GIM predicted values is always within 4 °C which is close to the accuracy of the experiment.

4.2. Stoichiometry variation

The molar ratio of amine to epoxy groups in a given mixture affects the reactions which occur during cure, the stoichiometry of the cured network and hence the final properties of the resin. In theory, resins cured with a 1:1 stoichiometric ratio of amine hydrogen to epoxy

Table 2
Experimental and GIM beta and glass transition temperatures at three frequencies for DGEBA cured with 33DDS and 44DDS. The amine/epoxy ratio is 1:1.1. Errors quoted are the standard deviation of the sample range. Where error values are absent, there was no deviation in the measurements.

Frequency (Hz)	DGEBA/33DDS			
	Exp. T_β (°C)	GIM T_β (°C)	Exp. T_g (°C)	GIM T_g (°C)
1	−59 ± 1	−58	172 ± 1	176
5	−49	−47	177 ± 1	179
10	−45	−42	179 ± 1	181
	DGEBA/44DDS			
	Exp. T_β (°C)	**GIM T_β (°C)**	**Exp. T_g (°C)**	**GIM T_g (°C)**
1	−48 ± 2	−49	199 ± 1	199
5	−39 ± 3	−38	205 ± 1	202
10	−35 ± 4	−32	208 ± 1	204

groups have the ideal number of reactants and under ideal conditions would be anticipated to produce cured resins with the best available properties. The properties in question would be those which 'improve' with increasing cure, such as glass transition temperature, stiffness and strength. Inevitably, it is likely that increased cure would be detrimental to other important properties, such as fracture toughness.

The assumption that stoichiometry leads to ideal properties relies on assuming that the different curing reactions are equally likely to occur and that the entire mixture can react without any reactants becoming trapped in the growing network structure. In reality, neither of these is the case for two reasons. Firstly, at the beginning of the cure, the primary amine – epoxy reaction is the only reaction which can occur and also this reaction is more likely to occur compared to the secondary amine – epoxy reaction once the cure has started. Secondly, the maximum achievable degree of cure is less than 100% as some unreacted species will always become caught in the polymer structure unable to react with each other, particularly where crosslinking is prevalent such as in amine cured epoxy resins. However, a reduction in the modulus and the strength has been observed in structures with increased crosslink density [22]. This is due to the greater crosslink density restricting the molecules from filling free volume, which causes an increase in the distance between neighbouring chains and reduces the chances of intermolecular interactions. This effect has been observed in non-stoichiometric resins, where unreacted species fill the free volume, this enhances chain interactions and the result is an increased stiffness [23,24].

However, both these factors (and others which may result in non-stoichiometric resins) are likely to have an approximately equal influence when the variation of initial stoichiometry is limited to approximately ± 10% from the assumed ideal. On initial consideration, it might be anticipated that the 1:1 stoichiometric mixture would produce resins with the highest glass transition temperature, and the amine rich or epoxy rich mixtures would have lower values. Should this trend not be observed, it may indicate a preferential entrapment of certain chemical species which only occurs at particular amine/epoxy ratios or with particular isomers of the amine curing agent.

Comparisons of experimental and GIM predicted glass and beta transition temperatures for DGEBA/33DDS and DGEBA/44DDS as a function of both stoichiometry and frequency are provided in Figs. 6–9. The amine/epoxy ratio is varied from 1:0.9 to 1:1.1 in 0.05 steps.

There is good agreement between measured and predicted beta transition temperatures for DGEBA/33DDS as shown in Fig. 6. The differences between the experimental and GIM predicted peak temperatures are typically less than 4 °C, with the notable exception of the 1:1 ratio. The general trend observed in the beta transition temperatures is a curve with the amine and epoxy rich ratios having lower values than the more balanced mixtures between. However, in the 1:1 case, there is a clear dip in the beta transition temperature away from this trend.

In aromatic epoxy resins, the molecular relaxations, which are responsible for the beta transition, have a number of contributing mechanisms and therefore the transition temperature, magnitude and shape are dependent on several factors. These molecular motions can be broadly divided into two types. The first is a crankshaft style rotation of the hydroxy-propyl ether groups created as a result of the epoxide ring opening during cure. The second contribution is from the rotation of the

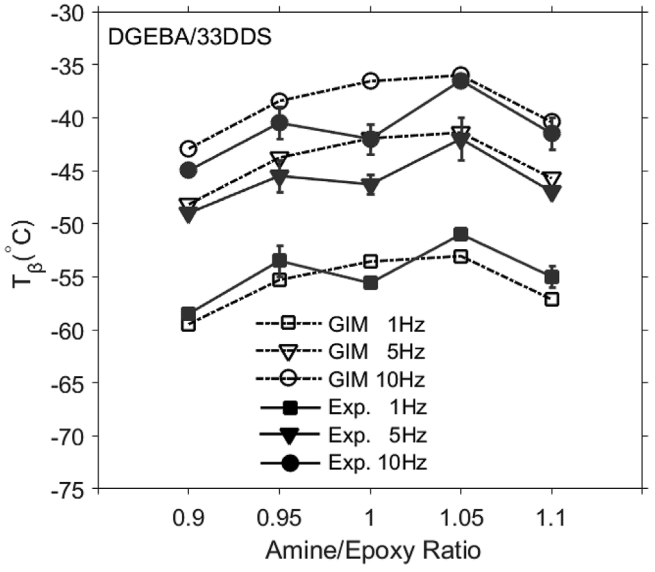

Fig. 6. Experimental and GIM beta transition temperatures as a function of amine/epoxy ratio at three frequencies for DGEBA cured with 33DDS. Errors quoted are the standard deviation of the sample range.

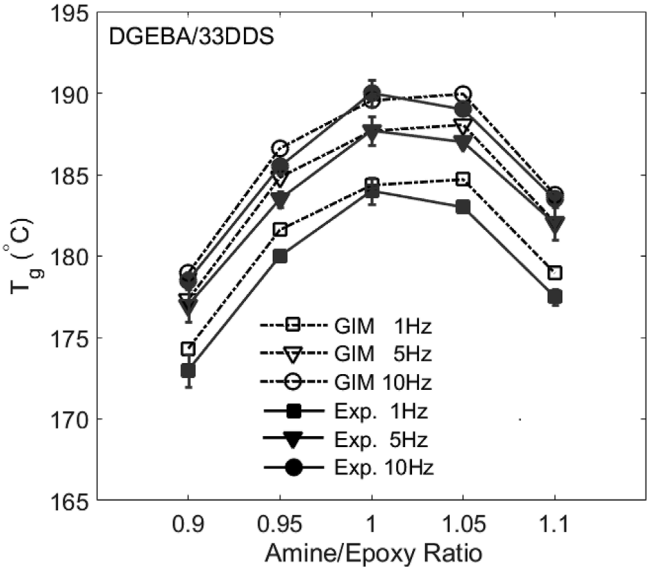

Fig. 7. Experimental and GIM glass transition temperatures as a function of amine/epoxy ratio at three frequencies for DGEBA cured with 33DDS. Errors quoted are the standard deviation of the sample range.

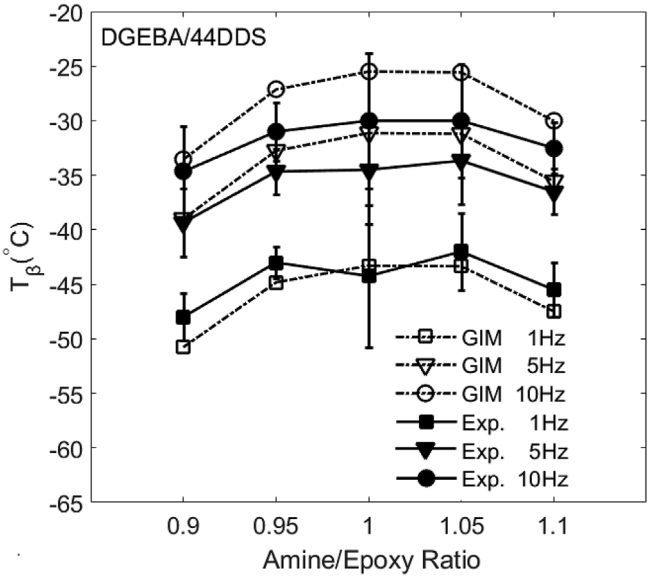

Fig. 8. Experimental and GIM beta transition temperatures as a function of amine/epoxy ratio at three frequencies for DGEBA cured with 44DDS. Errors quoted are the standard deviation of the sample range.

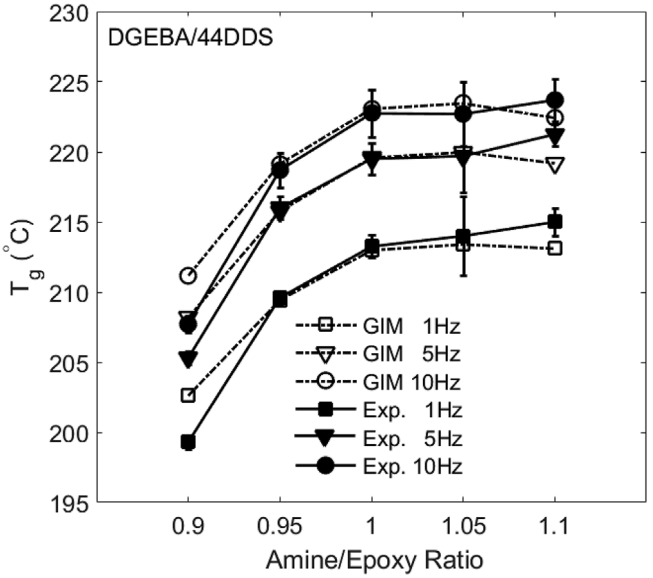

Fig. 9. Experimental and GIM glass transition temperatures as a function of amine/epoxy ratio at three frequencies for DGEBA cured with 44DDS. Errors quoted are the standard deviation of the sample range.

phenylene rings present in either the epoxy or amine parts of the network.

The cold side of the beta transition peak has been linked to the phenylene ring rotation in the epoxy mer units and the hot side of the peak has been linked to similar motions in the amine mer units. Changes in the beta transition temperature can therefore be caused by altering the energy required to perform the molecular motions described. It is unclear how this would be achieved for the hydroxyl-propyl ether mechanism but for the second mechanism, restricting phenylene ring rotation would increase the energy required to rotate the rings. Given there are multiple contributions to the beta transition, restriction of the phenylene ring rotation may or may not actually increase the overall beta transition temperature as the other influences may obscure any observable effect.

The magnitude of the beta transition can be increased by ensuring more of the functional groups responsible for the beta transition loss event are present in the cured resin. More hydroxyl-propyl ether groups will be present if the degree of cure is higher and more phenylene rings will be present by altering the reactant chemistry and/or stoichiometry. The shape of the beta transition is primarily a result of how the individual contributions from each mechanism sums to give an overall peak. In a system with multiple mechanistic contributions to the overall loss event, separating which of the individual effects are influencing the temperature and/or the magnitude of the transition is a non-trivial exercise.

The beta transition temperature reduction observed in the 1:1 resin must have been caused by a reduction in the energy required to initiate one of the molecular mechanisms described above. In a 1:1 stoichiometry, there are less unreacted species in the network so it seems likely that the presence of unreacted species in the non-stoichiometric 1:0.95 and 1:1.05 resins is interfering with the motions responsible for the beta transition. Correspondingly, once the ratio has reached either 1:0.9 or 1:1.1, the beta transition temperature drops again. This may be because the unreacted species in an only slightly non-stoichiometric resin are small enough to interfere, but in the more epoxy or amine rich ratios, the unreacted species are now too large or numerous to behave in the same way. The GIM implementation used in this work does not encapsulate this behaviour, as evidenced by the relative disparity between beta transition temperature values for the 1:1 resin in Fig. 6. However, the effect is small and is not anticipated to significantly impact on bulk property prediction.

A second feature of the beta transition temperature plots for DGEBA/33DDS as seen in Fig. 6, is that the 1:1 stoichiometric resin does not have the highest beta transition temperature. In the model predictions, there is a slight beta transition temperature increase as the amine/epoxy ratio is increased from 1:1 to 1:1.05 until it drops back down for 1:1.1. This trend is also observed in the experimental data but is less clear due to the previously discussed dip observed at 1:1. The reasons for this effect are not immediately clear and may simply be an artefact of the coarseness of the stoichiometry step chosen.

In contrast to the relative complexity described above, the effect of stoichiometry on the glass transition temperature in DGEBA/33DDS is relatively straightforward as seen in Fig. 7. There is very good agreement between the experimental and GIM predicted glass transition temperatures across a range of amine/epoxy ratios and frequencies. The typical difference between measured and predicted glass transition temperature is 3 °C or less. The highest glass transition temperature is observed in the 1:1 stoichiometric resin, with clear drops seen in both the amine and epoxy rich resins. This result suggests that, in DGEBA/33DDS, a stoichiometric ratio between epoxy and amine allows the formation of a higher crosslink density than for non-stoichiometric ratios.

The experimental and GIM predicted beta transition temperatures of DGEBA/44DDS as a function of amine/epoxy ratio and frequency are presented in Fig. 8. The agreement between measured and predicted beta transition temperatures has a greater variation for DGEBA/44DDS than for DGEBA/33DDS. Also, the reduction in beta transition temperature at 1:1 stoichiometry observed at all three frequencies for DGEBA/33DDS is now only seen in DGEBA/44DDS at 1 Hz. However, both of these observations may be a consequence of the larger errors associated with the experimental data for DGEBA/44DDS than those associated with DGEBA/33DDS.

The experimental and GIM predicted glass transition temperatures for DGEBA/44DDS as a function of amine/epoxy ratio and frequency are presented in Fig. 9. Again, the agreement between predicted and measured temperatures is good across the range of amine/epoxy ratios and frequencies. However, one disparity is the apparent increase in experimental glass transition temperature as the amine/epoxy ratio is increased beyond 1:1 stoichiometry. For DGEBA/44DDS, the highest glass transition temperatures are observed for the 1:1.1 ratio resin which contrasts with DGEBA/33DDS where the highest glass transition temperature is for the 1:1 resin.

It has been shown previously [14] that 33DDS cured triglycidyl-*meta*-aminophenol (TGMAP) has a lower crosslink density than the equivalent 44DDS cured resin. It was suggested this was due to a greater extent of the curing reaction occurring at the initial lower temperature dwell in the cure cycle for the 33DDS compared to the 44DDS. This was attributed to 33DDS being more reactive than 44DDS due to the meta positioning of the functional groups on the phenylene rings. In addition to this, the increased reactivity of 33DDS with DGEBA compared to 44DDS has also been reported previously [25].

This argument can be extended to account for the difference in the glass transition temperatures of DGEBA/33DDS and DGEBA/44DDS reported here. As shown earlier, DGEBA/44DDS has a higher glass transition temperature than DGEBA/33DDS which suggests it has a higher crosslink density too. Alongside this, an epoxy rich mixture leads to a slight increase in glass transition temperature for DGEBA/44DDS (Fig. 9) but a significant drop in glass transition temperature for DGEBA/33DDS (Fig. 7). This suggests that the excess epoxy is enhancing the development of linear chains in the DGEBA/33DDS network and in contrast, enhancing the development of crosslinks in the DGEBA/44DDS network. While the model captures the majority of the glass transition temperature against amine/epoxy ratio and frequency behaviour, the implementation used here does not entirely account for this effect. This results in the predicted glass transition temperature for DGEBA/44DDS reducing slightly at a ratio of 1:1.1 instead of the slight

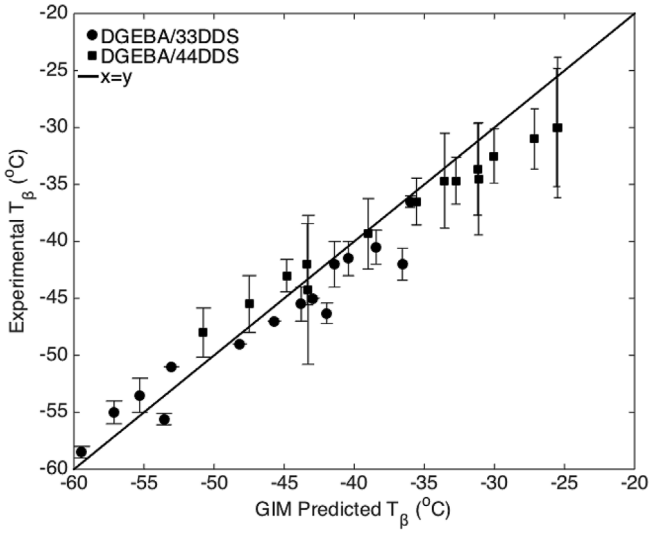

Fig. 10. Experimental versus GIM predicted beta transition temperatures for DGEBA/33DDS and DGEBA/44DDS. Data is presented for a range of amine/epoxy ratios from 1:0.9 to 1:1.1 and frequencies of 1, 5 and 10 Hz. The solid line is a linear correlation. Errors quoted are the standard deviation of the sample range.

increase seen experimentally.

Finally, the measured and predicted beta and glass transition temperatures from this and the previous section are plotted against each other in Figs. 10 and 11 to illustrate the overall accuracy of the model.

In both plots, the data points generally sit on or near the $x = y$ line confirming the overall very good agreement between the experimental data and GIM predictions. The accuracy of the predictions looks poorer for the beta transitions (Fig. 10) primarily due to the scale used in the plot. In summary, these comparisons confirm the model's ability to accurately predict both the high and low temperature transition temperatures for two epoxy resins cured with amines with subtly different chemical structure over a range of frequencies.

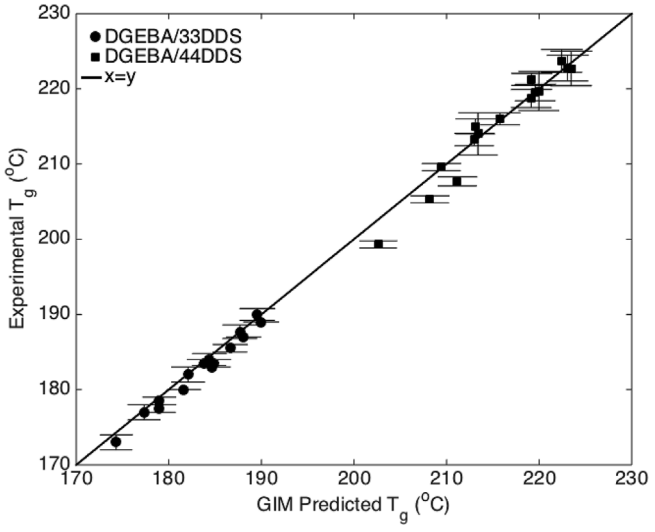

Fig. 11. Experimental versus GIM predicted glass transition temperatures for DGEBA/33DDS and DGEBA/44DDS. Data is presented for a range of amine/epoxy ratios from 1:0.9 to 1:1.1 and frequencies of 1, 5 and 10 Hz. The solid line is a linear correlation. Errors quoted are the standard deviation of the sample range.

Table 3
Experimental and GIM room temperature densities for DGEBA cured with 33DDS and 44DDS. The amine/epoxy ratio is 1:1.1. Errors quoted are the standard deviation of the sample range.

DGEBA/33DDS Density (g.cm^{-3})		DGEBA/44DDS Density (g.cm^{-3})	
Exp.	GIM	Exp.	GIM
1.2417 ± 0.0004	1.247	1.2400 ± 0.0004	1.240

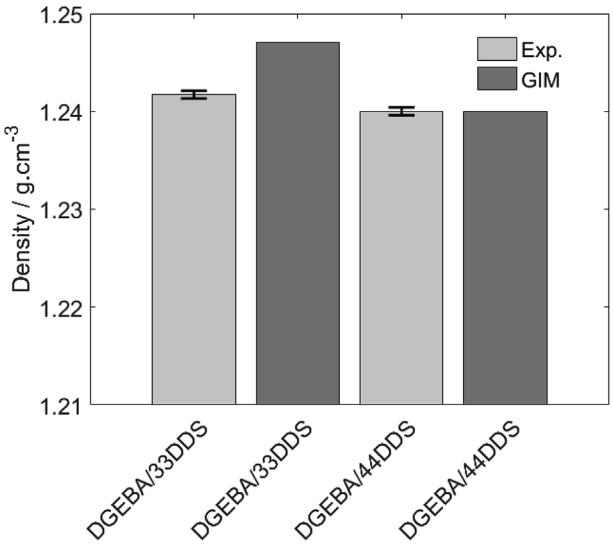

Fig. 12. Experimental and GIM room temperature densities DGEBA/33DDS and DGEBA/44DDS. The amine/epoxy ratio is 1:1.1. Errors quoted are the standard deviation of the sample range.

4.3. Density

The experimental and GIM predicted room temperature densities are compared in Table 3 and shown graphically in Fig. 12 for DGEBA/33DDS and DGEBA/44DDS. The agreement between the measured and predicted densities is excellent for DGEBA/44DDS whilst a small overestimation is observed for DGEBA/33DDS.

The packing efficiencies of *meta* substituted phenylene rings are often lower than those of the equivalent *para* substituted isomers. This manifests in the melting point of pure 33DDS being slightly lower than the melting point of 44DDS; the latter can pack more efficiently due to the *para* arrangement of the substituents on the phenylene ring. However, in aromatic amine cured epoxy resins, the reverse is often true. It has been shown in both DGEBA [12] and TGAP [14] cured with 33DDS and 44DDS that the density is higher in the *meta* 33DDS cured resin. Furthermore, the position of the functional groups on the epoxy follows a similar trend as those on the amine. The *meta* version of TGAP (TGMAP) has a higher density when cured with either 33DDS or 44DDS when compared to the *para* equivalent (TGPAP) [14].

In a highly crosslinked epoxy with a typical network structure, it is reasonable to assume that having substituents on the phenylene ring in the *para* arrangement forces the structure to adopt a more linear structure leaving larger areas of free volume. With the ring substituents in the *meta* arrangement, the extra conformational freedom available to each amine mer unit on the polymer chain is apparently enough to improve the space filling efficiency to such an extent that the cured resin's density is higher. Previous work has used positron annihilation lifetime spectroscopy (PALS) to show that the free volume differs in resins cured using the two DDS isomers [25]. The PALS measurements showed the average free volume hole size reduces from 82 to 76 Å^3 on going from DGEBA/44DDS to DGEBA/33DDS, which is consistent with the observed densities reported here. The model is capable of

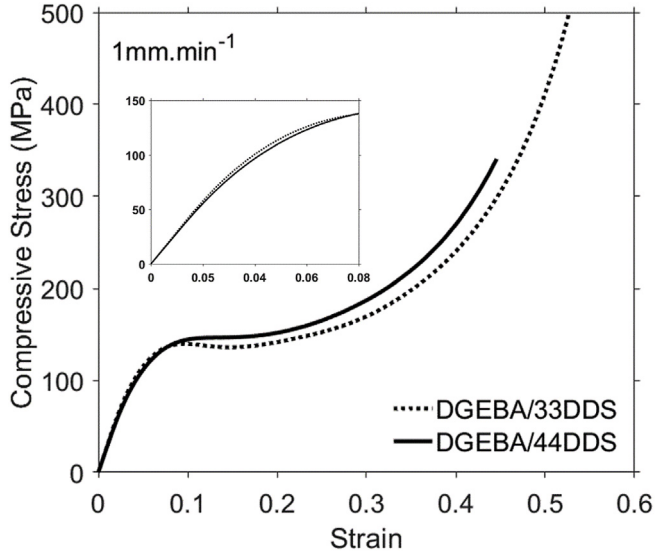

Fig. 13. Experimental room temperature compressive stress-strain curves for DGEBA cured with both 33DDS and 44DDs at 1 mm.min-1 strain rate. The amine/epoxy ratio is 1:1.1.

reproducing this behaviour despite having the same van der Waal's volume input parameter (see Table 1) for both isomers. The actual volume of the 33DDS cured resin is modelled as a function of temperature and, at room temperature where the density is recorded, the resin volume in DGEBA/33DDS is lower than in DGEBA/44DDS. This is a direct consequence of the slightly decreased magnitude of the beta transition in the former compared to the latter (see Fig. 5).

4.4. Compressive stress-strain curves

The experimental room temperature compressive stress-strain curves for both DGEBA/33DDS and DGEBA/44DDS are shown in Fig. 13 for a strain rate of 1 mm.min^{-1}. Similar stress-strain curves were measured at strain rates of 5 and 10 mm.min^{-1} for both resins but these are qualitatively very similar and are therefore presented in the supplementary information.

In the initial elastic part of the curve, DGEBA/33DDS has a higher gradient and therefore stiffness than DGEBA/44DDS. The higher compressive modulus for DGEBA/33DDS is consistent with the higher density observed in the previous section. More material is present to support the load and there are more intermolecular interactions between the polymer chains so the stiffness is higher. This behaviour is very similar to that observed in TGMAP/TGPAP cured with 33DDS and 44DDS [14]. However, the yield strength reported here is lower in the *meta* substituted DGEBA/33DDS which is in contrast to that reported for the *meta* substituted epoxy or amine in TGAP/DDS. In DGEBA/44DDS the onset of strain hardening post-yield may be interfering with the measurement of the yield point. The stress-strain curve is particularly flat around the yield point for this particular resin.

After the yield point, the curves have swapped and now the DGEBA/44DDS is able to support more stress than DGEBA/33DDS. This result is in contrast to previous results for TGAP/DDS and suggests that internal antiplasticisation is either more complicated in DGEBA/DDS resins or not present. The DGEBA/33DDS has a higher stress and strain at failure which confirms the lower degree of crosslinking in this resin. At higher applied stresses, a lower number of crosslinks allows the applied stress to be accommodated in the structure by compressing the polymer chains. With more crosslinks present, such as in DGEBA/44DDS, the structure has less available compression before the crosslinks are required to break to accommodate the applied stress, resulting in a lower failure stress/strain.

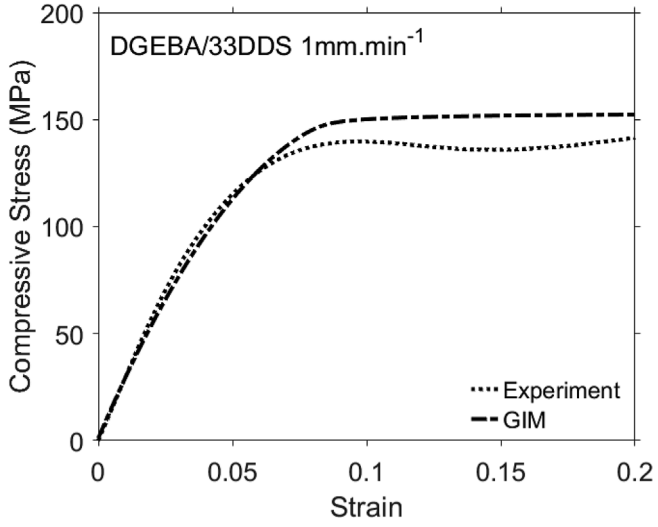

Fig. 14. Experimental and GIM room temperature compressive stress-strain curves for DGEBA cured with 33DDS measured at room temperature and a strain rate of 1 mm.min^{-1}. The amine/epoxy ratio is 1:1.1.

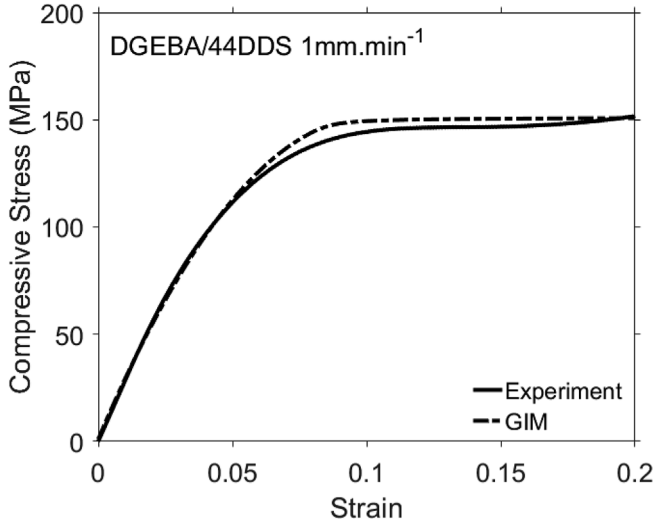

Fig. 15. Experimental and GIM room temperature compressive stress-strain curves for DGEBA cured with 44DDS measured at room temperature and a strain rate of 1 mm.min^{-1}. The amine/epoxy ratio is 1:1.1.

Comparisons of the experimental and GIM predicted room temperature compressive stress-strain curves for a strain rate of 1 mm.min^{-1} are shown in Figs. 14 and 15. Again, similar comparisons for 5 and 10 mm.min^{-1} are qualitatively similar and are provided in the supplementary data. The agreement between the measured and predicted curves is very good, particularly in the initial elastic region. There is some disparity in the predicted and measured yield strength for DGEBA/33DDS, but the accuracy is improved in DGEBA/44DDS. As a result of the former, the model does not entirely capture any possible internal antiplasticisation behaviour observed experimentally. There is also good agreement between the measured and predicted curves for the 5 and 10 mm.min^{-1} strain rates.

Finally, the experimental and GIM predicted room temperature compressive modulus and yield strengths of DGEBA/33DDS and DGEBA/44DDS are compared in Figs. 16 and 17. The agreement between measured and predicted values is generally good, although there are some discrepancies in the yield strength for DGEBA/33DDS again.

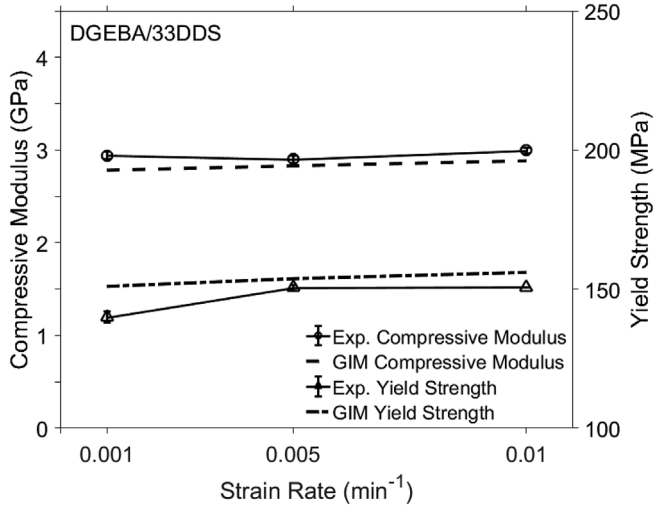

Fig. 16. Experimental and GIM room temperature compressive modulus and yield strength as a function of strain rate for DGEBA cured with 33DDS. The amine/epoxy ratio is 1:1.1. Errors quoted are the standard deviation of the sample range.

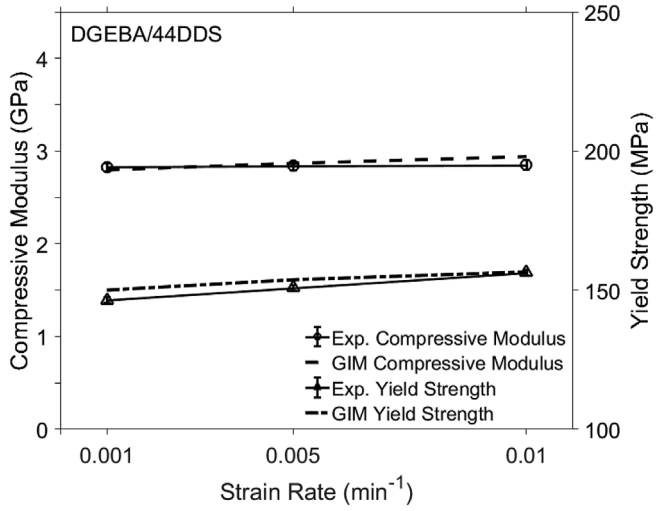

Fig. 17. Experimental and GIM room temperature compressive modulus and yield strength as a function of strain rate for DGEBA cured with 44DDS. The amine/epoxy ratio is 1:1.1. Errors quoted are the standard deviation of the sample range.

5. Conclusions

The thermo-mechanical properties of a difunctional epoxy resin cured with two isomeric diamines have been predicted using Group Interaction Modelling and also determined experimentally. The model has accurately predicted the properties of DGEBA cured with both the *meta* and *para* isomers of DDS (33DDS and 44DDS). The loss tangent versus temperature profiles have been modelled, correctly reproducing the major loss events such as the beta and glass transitions. The predicted transition temperatures are accurate for both diamine isomers and over a range of frequencies. Varying the amine/epoxy ratio results in subtle changes in the transitions, most of which are captured by the model. Alongside this, the density and compressive stress-strain curves of the cured resins have been predicted and measured experimentally with good agreement between the two.

The interpretation of the both the modelling and experimental data has concentrated on the differences in the resin as a result of curing with the two diamine isomers. In 33DDS, the substituents on the phenylene ring are in a *meta* arrangement which results in a structure with more conformational freedom which increases packing efficiency and therefore density and compressive modulus. The non-linear structure also contributes to the lower glass transition temperature in DGEBA/33DDS. The reactivity of the *meta* 33DDS is higher than the *para* 44DDS which results in more linear chains in DGEBA/33DDS than DGEBA/44DDS. This also contributes to a lower glass transition temperature in DGEBA/33DDS than DGEBA/44DDS. The factors governing the beta transition of both diamine isomers have been rationalised in terms of the molecular level mechanisms which dissipate energy at low temperatures.

The results and interpretation presented here illustrate the complexity of the relationship between the chemical structure and thermo-mechanical properties in amine cured epoxy resins. By using a carefully chosen, subtly different pair of resins as the basis for both modelling and experimental measurements, the factors governing the properties of such resins have been illustrated and explained. The model itself is a step forward in our ability to calculate properties of complex polymeric structures. It has proven accurate in predicting a variety of experimentally verifiable properties as a function of temperature, strain rate, strain, resin chemistry and resin stoichiometry. In particular, the model represents an opportunity to push forward the development of new and improved high performance epoxy resins for use in the aerospace and automotive industries.

Conflicts of interest

None.

Funding sources

This work was supported by the Air Force Office of Scientific Research, Air Force Material Command, USAF [FA9550-15-1-0246] and by the UK Engineering and Physical Sciences Research Council [EP/M508135/1].

Acknowledgements

The authors gratefully acknowledge Huntsman Advanced Materials for supplying the 33DDS (Aradur 9719-1) hardener used in this study.

Appendix A. Supplementary data

Supplementary data to this article can be found online at https://doi.org/10.1016/j.polymer.2018.10.016.

References

[1] D. Porter, Group Interaction Modelling of Polymer Properties, CRC Press, 1995.
[2] D. Porter, P.J. Gould, A general equation of state for polymeric materials, J. Phys. IV 134 (2006) 373–378.
[3] D. Porter, P.J. Gould, Predictive nonlinear constitutive relations in polymers through loss history, Int. J. Solid Struct. 46 (9) (2009) 1981–1993.
[4] D. Porter, F. Vollrath, Z. Shao, Predicting the mechanical properties of spider silk as a model nanostructured polymer, Eur. Phys. J. E 16 (2) (2005) 199–206.
[5] J.P. Foreman, et al., Rate dependent multiscale modelling of fibre reinforced composites, Plast. Rubber Compos. 38 (2–4) (2009) 67–71.
[6] J.P. Foreman, et al., Hierarchical modelling of a polymer matrix composite, J. Mater. Sci. 43 (20) (2008) 6642–6650.
[7] J.P. Foreman, et al., Multi-scale modelling of the effect of a viscoelastic matrix on the strength of a carbon fibre composite, Phil. Mag. 90 (31–32) (2010) 4227–4244.
[8] J.P. Foreman, et al., A model for the prediction of structure–property relations in cross-linked polymers, Polymer 49 (25) (2008) 5588–5595.
[9] J.P. Foreman, et al., Predicting the thermomechanical properties of an epoxy resin blend as a function of temperature and strain rate, Compos. Appl. Sci. Manuf. 41 (9) (2010) 1072–1076.
[10] H.P. Liu, A. Uhlherr, M.K. Bannister, Quantitative structure-property relationships for composites: prediction of glass transition temperatures for epoxy resins, Polymer 45 (6) (2004) 2051–2060.
[11] N.T. Guest, et al., Characterization and modeling of diglycidyl ether of bisphenol-a epoxy cured with aliphatic liquid amines, J. Appl. Polym. Sci. 130 (5) (2013)

3130–3141.
[12] A.C. Grillet, et al., Mechanical and viscoelastic properties of epoxy networks cured with aromatic diamines, Polymer 32 (10) (1991) 1885–1891.
[13] J.W. Tu, et al., Phenylene ring motions in isomeric glassy epoxy networks and their contributions to thermal and mechanical properties, Macromolecules 48 (6) (2015) 1748–1758.
[14] R. Ramsdale-Capper, J.P. Foreman, Internal antiplasticisation in highly crosslinked amine cured multifunctional epoxy resins, Polymer 146 (2018) 321–330.
[15] D. Porter, Materials modelling: a bridge from atoms to bulk properties, Adv. Perform. Mater. 3 (3–4) (1996) 309–324.
[16] J.P. Foreman, et al., Thermodynamic and mechanical properties of amine-cured epoxy resins using group interaction modelling, J. Mater. Sci. 41 (20) (2006) 6631–6638.
[17] S. Behzadi, F.R. Jones, Yielding behavior of model epoxy matrices for fiber reinforced composites: effect of strain rate and temperature, J. Macromol. Sci. Phys. B44 (6) (2005) 993–1005.
[18] H. Eyring, Viscosity, plasticity, and diffusion as examples of absolute reaction rates, J. Chem. Phys. 4 (4) (1936) 283–291.
[19] J.D. Ferry, H.S. Myers, Viscoelastic properties of polymers, J. Electrochem. Soc. 108 (7) (1961).
[20] C. Bauwens-Crowet, The compression yield behaviour of polymethyl methacrylate over a wide range of temperatures and strain-rates, J. Mater. Sci. 8 (7) (1973) 968–979.
[21] J. Bicerano, Prediction of Polymer Properties, Marcel Dekker, New York, 1993.
[22] E. Morel, et al., Structure-properties relationships for densely cross-linked epoxide-amine systems based on epoxide or amine mixtures, J. Mater. Sci. 24 (1) (1989) 69–75.
[23] S. Pandini, et al., Thermomechanical and large deformation behaviors of anti-plasticized epoxy resins: effect of material formulation and network architecture, Polym. Eng. Sci. 57 (6) (2017) 553–565.
[24] G.R. Palmese, R.L. Mccullough, Effect of epoxy amine stoichiometry on cured resin material properties, J. Appl. Polym. Sci. 46 (10) (1992) 1863–1873.
[25] M. Jackson, et al., Effect of free volume hole-size on fluid ingress of glassy epoxy networks, Polymer 52 (20) (2011) 4528–4535.